

## MEASUREMENT OF DIJET PRODUCTION AT LOW $Q^2$ AT HERA

KAMIL SEDLÁK

(on behalf of the H1 collaboration)

*Institute of Physics ASCR*

*Na Slovance 2, 182 21 Praha 8, Czech Republic*

*E-mail: ksedlak@fzu.cz*

A recent H1 measurement [1] of triple differential dijet cross sections in  $e^\pm p$  interactions in the region of photon virtualities  $2 < Q^2 < 80 \text{ GeV}^2$  is presented and compared to LO and NLO QCD predictions. Effects that go beyond the fixed-order NLO QCD calculations are identified.

### 1 Introduction

Jet cross sections in electron-proton collisions are successfully described by next-to-leading order (NLO) QCD calculations in most of the HERA kinematic range. However, regions of phase space have previously been observed for which NLO predictions do not reproduce the data satisfactorily [2] and leading order (LO) Monte Carlo simulations with different approaches to modelling higher order QCD effects are often more successful.

In this analysis we focus on the dijet cross section in a region where we expect large deviations between measurement and the QCD predictions. This kinematic region is characterised by low photon virtualities,  $Q^2$ , forward jet pseudorapidities,  $\eta^*$ , and high inelasticities,  $y$ , (which corresponds to the region of low  $x_\gamma^{\text{jets}}$ , the fraction of the photon four-momentum carried by the parton involved in the hard scattering).

The analysis is described in much more detail in a recent H1 publication [1]. Here we just recall its most important results, and in addition present one particular aspect of the analysis, namely an unphysical dependence of the NLO QCD predictions calculated using the program JETVIP [3] on a technical parameter  $y_c$ . Figure 2, showing the problematic  $y_c$  dependence, is the only result which is not included in [1].

### 2 Data samples and event selection

The present analysis is based on a  $57 \text{ pb}^{-1}$  data sample taken in the years 1999 and 2000 with  $\sqrt{s} = 318 \text{ GeV}$ . The kinematic region is defined by the cuts:  $2 < Q^2 < 80 \text{ GeV}^2$ ;  $0.1 < y < 0.85$ ;  $E_{T1}^* > 7 \text{ GeV}$ ;  $E_{T2}^* > 5 \text{ GeV}$ ;  $-2.5 < \eta_1^* < 0$ ;  $-2.5 < \eta_2^* < 0$ , where jet transverse energies,  $E_T^*$ , and pseudorapidities,  $\eta^*$ , are calculated relative to the  $\gamma^*p$  collision axis in the  $\gamma^*p$  centre-of-mass frame. The jets are ordered according to their transverse energy, with jet 1 being the highest  $E_T^*$  jet. The dijet cross sections are presented as a function of the variable  $x_\gamma^{\text{jets}}$  defined by eq. (1) of [4].

### 3 Results

Triple differential dijet cross section is presented as a function of  $x_\gamma^{\text{jets}}$  in different bins of  $Q^2$  and  $E_T^*$  in Fig. 1. The variable  $E_T^*$  denotes the transverse energies of the jets with the highest and second highest  $E_T$ , so that each event contributes twice to the distributions, not necessarily in the same bin. The data are compared with the NLO direct photon calculations performed with DISENT and JETVIP. The uncertainties from variations of the factorisation and renormalisations scales<sup>a</sup> in the interval  $\mu/2$  to  $2\mu$ , as well as from hadronisation corrections, are illustrated.

Figure 1 demonstrates that the NLO direct photon calculations describe the data in the region of high  $x_\gamma^{\text{jets}}$ , where direct photon interactions dominate. For  $x_\gamma^{\text{jets}} < 0.75$ , the description is nowhere perfect, indicating the need for orders beyond NLO. The description of the data for  $x_\gamma^{\text{jets}} < 0.75$  gets worse as  $Q^2$  and  $E_T^*$  decrease. The discrepancy is particularly pronounced at small  $x_\gamma^{\text{jets}}$ , low  $Q^2$  and low  $E_T^*$ , where the data lie significantly above the theoretical predictions, even taking into account the sizable scale uncertainty.

The discrepancy between DISENT and JETVIP direct photon predictions in Fig. 1 is observed only for multi-differential distributions which include a jet variable. It gets substantially smaller for the inclusive dijet cross section  $d^2\sigma_{\text{ep}}/dQ^2 dy$  [5] and agrees within 2% for the total dijet cross section in our kinematic region.

The pattern of the observed discrepancy between the data and the NLO direct photon calculations in Fig. 1 suggests an explanation in terms of the interactions of resolved virtual photons, understood as an approximation to contributions beyond NLO. Of the NLO parton level calculations, only JETVIP includes a resolved virtual photon contribution. Once it is included, the NLO prediction gets closer to the data, though there is still a discrepancy between the data and the calculations at low to moderate  $x_\gamma^{\text{jets}}$  and low  $Q^2$ .

Unfortunately, there is a large dependence of the NLO resolved photon contribution calculated by JETVIP on the slicing parameter<sup>b</sup>  $y_c$ . The resulting JETVIP predictions are therefore less reliable. The  $y_c$  dependence of the dijet cross section predicted by JETVIP is shown in different bins of  $Q^2$  and  $E_T^*$  in Fig. 2. For  $10^{-5} < y_c < 10^{-3}$ , the  $y_c$  range recommended [3] by the authors of JETVIP, the NLO direct photon predictions are much more stable than those for the NLO resolved photon contribution. In the absence of other calculations of this kind, the data in Fig. 1 were compared with the results of the full JETVIP calculations using  $y_c = 0.003$ .

Unlike the parton level calculations, DISENT and JETVIP, LO MC models take into account initial and final state QCD parton showers. With the help of the HERWIG MC we show in [1] that these effects significantly increase the dijet cross section in our kinematic region, especially in the region of low  $Q^2$ , low  $E_T^*$  and low  $x_\gamma^{\text{jets}}$ . We also indicate the effects of resolved photons with longitudinal polarisation. Once they are included, the prediction of the MC program HERWIG provides a better description of the data (see figures and discussion in [1]).

<sup>a</sup> $E_{T1}^*$  is taken as the renormalisation scale, see [1] for the factorisation scale.

<sup>b</sup> $y_c$  is just a technical parameter used internally in JETVIP for numerical integration.

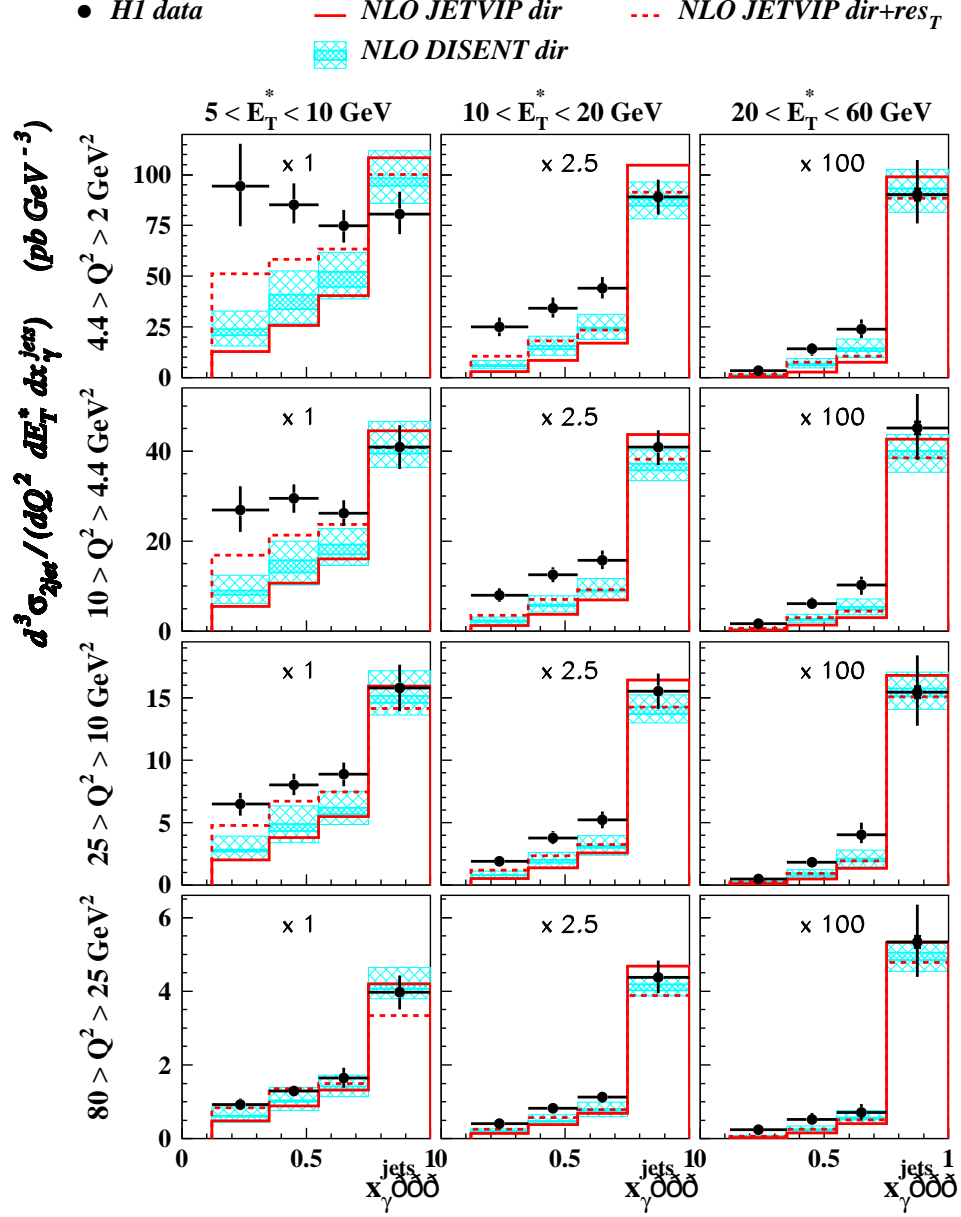


Figure 1. Triple differential dijet cross section  $d^3\sigma_{2jet}/dQ^2 dE_T^* dx_\gamma^{jets}$  with asymmetric  $E_T^*$  cuts (see text). The inner error bars on the data points show the statistical error, the outer error bars show the quadratic sum of systematic and statistical errors. Also shown are NLO direct photon calculations using DISENT (hatched area) and JETVIP (full line), as well as the sum of NLO direct and NLO resolved photon contributions from JETVIP (dashed line). All calculations are corrected for hadronisation effects. The inner hatched area illustrates the uncertainty due to the hadronisation corrections. The outer hatched area shows the quadratic sum of the errors from hadronisation and the scale uncertainty (shown only for DISENT). The scale factors applied to the cross sections are given.

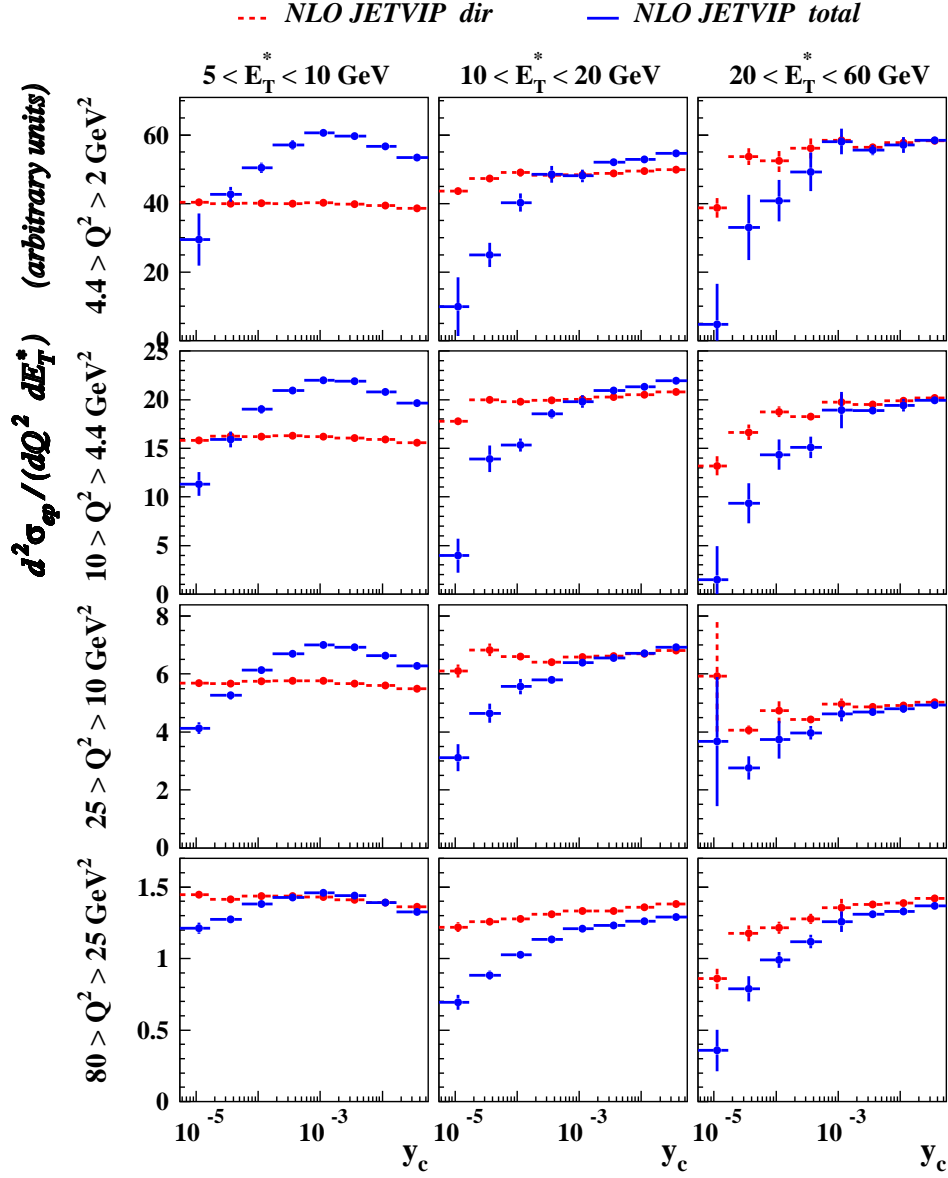


Figure 2. Dependence of dijet cross section  $d^2\sigma_{2jet}/dQ^2dE_T^*$  computed using JETVIP on the parameter  $y_c$ . The dotted points show the NLO direct photon contribution, while the full points are the complete NLO JETVIP prediction including the NLO resolved photon contribution. The former corresponds to the full points in Fig. 1, the latter to the dashed points in Fig. 1.

The MC program CASCADE [6] (not shown), which is based on the CCFM evolution scheme and unintegrated proton parton densities, describes the main qualitative trends in the data except the  $Q^2$  dependence. The overall quantitative description of the data is however worse than that by the full HERWIG MC.

#### 4 Conclusions

The recent H1 measurement of dijet cross section in the low  $Q^2$  region show clear evidence for effects that go beyond fixed-order NLO QCD calculations. The improved description of the data when including QCD parton showers and resolved photon contributions with longitudinal polarisation is illustrated in [1].

#### References

1. A. Aktas *et al.* [H1 Collaboration], Submitted to Eur.Phys.J. **C**, [hep-ex/0401010].
2. S. Chekanov *et al.* [ZEUS Collaboration], Eur. Phys. J. C **35** (2004) 487 [hep-ex/0404033].
3. B. Pötter, Comput. Phys. Commun. **119** (1999) 45 [hep-ph/9806437];  
B. Pötter, Comput. Phys. Commun. **133** (2000) 105 [hep-ph/9911221].
4. M. Lightwood “Dijet Production in DIS and Photoproduction”, *these proceedings*.
5. K. Sedláč, “Measurement of Dijet Production at Low  $Q^2$  at HERA”, Ph.D. Thesis, <http://www-h1.desy.de/psfiles/theses/h1th-336.ps>.
6. H. Jung and G. P. Salam, Eur. Phys. J. C **19** (2001) 351 [hep-ph/0012143];  
H. Jung, Comput. Phys. Commun. **143** (2002) 100 [hep-ph/0109102];  
H. Jung, tion,” Phys. Rev. D **65** (2002) 034015 [hep-ph/0110034].